JOURNAL OF Materials CHEMISTRY

Preparation of a Mott insulator based on a BEDT-TTF charge transfer complex of hydrogen cyananilate: α′-(BEDT-TTF)$_2$HCNAL

Md. B. Zaman,[a] J. Toyoda,[b] Y. Morita,[b] S. Nakamura,[b,c] H. Yamochi,*[c,d] G. Saito,*[c] K. Nishimura,[e] N. Yoneyama,[e] T. Enoki[e] and K. Nakasuji*[b]

[a]*Department of Structural Molecular Science, The Graduate University for Advanced Studies, Myodaiji, Okazaki 444-8585, Japan*
[b]*Department of Chemistry, Graduate School of Science, Osaka University, Toyonaka, Osaka 560-0043, Japan*
[c]*Chemistry Division, Graduate School of Science, Kyoto University, Kyoto, 606-8502, Japan*
[d]*CREST, Japan Science and Technology Corporation (JST), Japan*
[e]*Department of Chemistry, Graduate School of Science and Engineering, Tokyo Institute of Technology, Ookayama, Meguro-ku, Tokyo 152-8551, Japan*

Received 20th February 2001, Accepted 14th May 2001
First published as an Advance Article on the web 8th June 2001

BEDT-TTF (ET) and cyananilic acid (H_2CNAL) afforded charge transfer crystals by a diffusion method. The chemical formula of the complex was deduced based on all the information concerning the elemental, structural, electric, magnetic and optical analyses. The ET molecules form one-dimensional columnar stacks composed of twisted dimers with a face-to-face overlap (α′-type stack). The acid works as an oxidant and is deprotonated to form the monoanion, $HCNAL^{1-}$, which forms ribbon-like aggregation by means of hydrogen-bonds. The ribbons form anion layers that sandwich the ET layer. The crystal is semiconductive with a room temperature conductivity of 0.20–0.83 Scm^{-1} and activation energy of 0.15 eV along the stacking direction, though the band calculation by the extended Hückel method suggests a metallic nature, indicating strong electron-correlation in this system. The complex is a Mott insulator and its magnetic susceptibility is described by the one-dimensional $S=\frac{1}{2}$ antiferromagnetic Heisenberg chain model with $J/k_B=-52\pm3$ K.

1 Introduction

Bis(ethylenedithio)tetrathiafulvalene (BEDT-TTF or ET, Chart 1) has afforded a variety of charge-transfer (CT) complexes because of its structural and electronic features.[1] More than fifty two-dimensional (2D) superconductors have so far been prepared. The high T_c ET superconductors, such as κ-$(ET)_2X$ [X = $Cu(NCS)_2$, $Cu[N(CN)_2]Br$, $Cu[N(CN)_2]Cl$, $Cu(CN)[N(CN)_2]$] ($T_c=10-13$ K), are located in their electronic features between good metals, such as β-$(ET)_2I_3$, and Mott insulators, such as β′-$(ET)_2X$ (X = BrICl, ICl_2).[2] An intriguing feature of the Mott insulator κ-$(ET)_2Cu_2(CN)_3$, which is located in the proximate neighbor of the 10 K class superconductors, is that it is transformed into a superconductor by the application of pressure ($T_c=3.5$ K)[3] or by slight modification of the counter anion ($T_c=3$–10 K).[4]

Most of these complexes are composed of a combination of partially charged, mainly $+\frac{1}{2}$, ET molecules and closed-shell inorganic counter anions. Besides the inorganic anions, a variety of organic ones have been developed for conductive or magnetic ET complexes because of their easily designed molecular and electronic structures.[5] Among them polycyanocarbons,[5] polyfluoroalkanes[6] and polynitrophenols[7] have afforded interesting materials, such as organic metals, superconductors, Mott insulators, *etc.*

Polynitrophenols and other kinds of compounds containing hydroxide or amino groups, such as squaric acid, rhodizonic acid,[8] dimethylglyoxime,[9] biimidazole,[10] *etc.* are of interest from the viewpoints of the band filling control of organic conductors since they have different kinds of ionized species. Some of the haloanilic acids (chloranilic, bromanilic, Chart 1) have been used in the formation of organic metals with BEDO-TTF in which they exist as monoanionic species.[11] Among the anilic acids, nitranilic and cyananilic acid (2,5-dicyano-3,6-dihydroxy-*p*-benzoquinone, H_2CNAL) are some of the strongest electron acceptors, as well as being Brönsted acids bearing hydrogen-bonding sites. H_2CNAL is a flat molecule and may have a variety of species differing in the number of protons (H_nCNAL, $n=0$–4) and the charge (H_nCNAL$^{\delta}$, mainly $-2\leqslant\delta\leqslant0$). Recently, we have reported a 1D antiferromagnetic CT salt of tetramethyl-TTF (TMTTF); $(TMTTF)_2$HCNAL, in which H_2CNAL is deprotonated to

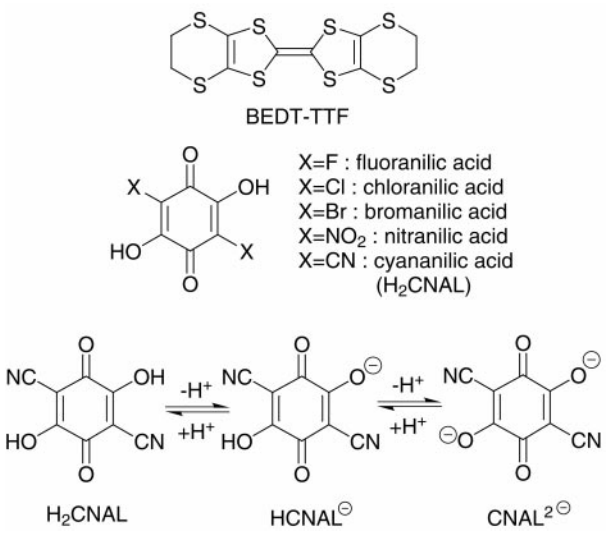

Chart 1 Compounds discussed in the text.

DOI: 10.1039/b101635k

produce $HCNAL^{1-}$ during the preparation.[12] In this report, the preparation, crystal structure and physical properties of a new Mott insulator α′-$(ET)_2HCNAL$ are described.

2 Experimental

H_2CNAL was prepared according to the procedure reported in the literature.[13] ET and H_2CNAL (0.05 mmol each) were each placed at the bottom of a chamber of an H-shaped cell. Diffusion of the starting materials in 12 mL of the mixed solvent (benzonitrile–CS_2 = 2 : 1) at room temperature for 1 to 4 weeks afforded black plates (mp 254–255 °C (decomp.)) of which only few were suitable for X-ray analysis. Anal. Found: C, 35.26; H, 1.79; N, 3.03%. Calcd for $(ET)_2HCNAL$ ($C_{28}H_{17}N_2O_4S_{16}$): C, 35.09; H, 1.79; N, 2.92%.

Optical measurements were carried out with a KBr disk on a Perkin-Elmer 1000 Series FT-IR (resolution 4 cm^{-1}) for IR and near-IR regions (400–7800 cm^{-1}) and on a Shimadzu UV-3100 spectrometer for near-infrared, visible and ultraviolet (UV–Vis–NIR) region (3800–42000 cm^{-1}).

DC conductivities of single crystals were measured by the standard four-probe method using gold wires of 10 μm in diameter with gold paste (Tokuriki, 8560-1A). EPR measurements were performed on a JEOL-TE200 X band ESR spectrometer with TE_{011} cavity whose temperature was varied from room temperature to 3 K by means of an Oxford ESR-910 cryostat. Static magnetic susceptibility was measured by the aid of a SQUID magnetometer (Quantum Design MPMS) from 300 K to 2 K.

X-Ray diffraction data were collected on an automated four-circle diffractometer (Rigaku AFC5R) with graphite monochromated Mo-Kα radiation at room temperature. All the calculations were performed using the teXsan crystallographic software package (Molecular Structure Corporation). The crystal structure was solved by direct methods (SHELXS86) and refined by full-matrix least squares (based on *F*). Although the differential synthesis gave the peak positions corresponding to all of the hydrogen atoms, the refinement of their positional parameters did not afford the appropriate values due to its small scattering factor. Hence, only their temperature factors were refined during a series of the least squares procedure, in which the positional and thermal parameters of non-hydrogen atoms were optimized, and then the positional parameters of hydrogen atoms were re-determined by the differential synthesis to be adopted in the next series of refinements. The site occupancy factor of the phenolic hydrogen was assumed to be 0.5 and was not refined.

Band structure was calculated based on the crystal structures at room temperature by extended Hückel tight-binding method with single-ζ parameters.[14]

3 Results and discussion

3.1 Degree of charge transfer

The stoichiometry of the complex was deduced to be $(ET)_2X$ based on the elemental analysis, where X is either $H_2CNAL^{\delta-}$, $HCNAL^{(1+\delta')-}$ or $CNAL^{(2+\delta'')-}$.

The bond lengths of the ET molecules and UV–Vis–NIR absorption spectrum of the complex provide valuable information concerning the degree of CT and hence the nature of the acceptor species.

Fig. 1 shows the molecular structures of the donor and anion. From the bond lengths of ET, the charge (γ) on this molecules has been estimated adopting two methods. Guionneau *et al.* derived the equation $\gamma = 6.347 - 7.363[(b+c)-(a+d)]$, where *a*, *b*, *c*, and *d* are averaged lengths of the bonds shown in Fig. 1 (left) assuming this donor molecule has D_{2h} symmetry.[15] According to this procedure, γ is estimated as 0.52 ± 0.09 in the title complex. Another method compares each bond length *a* to

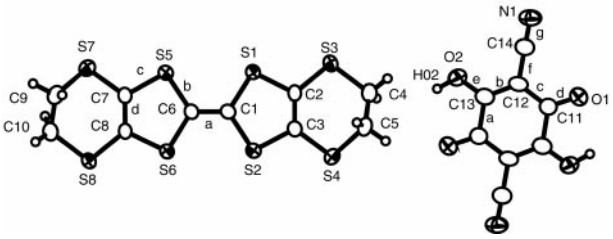

Fig. 1 The molecular plane projection of ET (left) and HCNAL (right) in the title complex. Assuming D_{2h} symmetry for the ET molecule, the averaged bond lengths are: $a = 1.362(5)$, $b = 1.736(2)$, $c = 1.750(2)$, $d = 1.332(4)$ Å. The site occupancy factor of the phenolic proton (H02) of HCNAL is assumed to be 0.5.

d with those in the ET molecules of known charges (0, $+\frac{1}{2}$, $+\frac{2}{3}$, $+1$, and $+2$).[16] This procedure explicitly revealed the inadequacy of using bond *d* in the estimation of γ, since the observed bond length of *d* (1.332(4) Å) is close to the neutral species (1.333(4) Å),[15] contrary to the optical and magnetic data of this complex which support substantially ionized nature of the ET molecules (*vide infra*). The evaluated γ values based on the bonds *a*, *b* and *c* are 0.58, 0.57 and 0.32, respectively, and that affords the averaged value of $\gamma = 0.49 \pm 0.2$.

For HCNAL, this anion showed a large deviation of bond lengths depending on the counter components in the complexes. The bond lengths in HCNAL in the several complexes in refs. 12 and 17 are: $a = 1.50(2)$–$1.54(2)$, $b = 1.38(2)$–$1.445(6)$, $c = 1.35(2)$–$1.43(1)$, $d = 1.21(1)$–$1.3(2)$, $e = 1.20(1)$–$1.31(1)$, $f = 1.40(2)$–$1.46(2)$, and $g = 1.1(1)$–$1.15(1)$ Å (for the definitions of *a*–*g*, see Fig. 1 (right)), within the range of which the bond lengths observed in the title complex are accommodated.

Fig. 2 compares the absorption spectrum of the complex (curve a) with that of $ET{\cdot}Br{\cdot}H_2O$ (curve b) in KBr. The absorption bands at 10–11×10^3 cm^{-1} (labeled band C) and 16–17×10^3 cm^{-1} (labeled band D) are due to the intramolecular transitions of an ET cation radical molecule; from the second HOMO to HOMO, and HOMO to LUMO, respectively.[16,18] The low energy CT transition (labeled band A) below 5×10^3 cm^{-1} is ascribed to an electronic transition either among the partially charged ET molecules or charge separated ET molecules and is commonly observed in highly conductive segregated materials. The optical transition between the fully ionized ET molecules appears at 5–6×10^3 cm^{-1} (labeled band B, indicated by an arrow), which is very weakly seen in curve a. It has been known that the intensity of band B decreases as the degree of ionicity of the ET molecule decreases from +1 in the segregated column and band B is nearly extinguished at +0.5.[19] Therefore, the weak appearance of the optical band B is indicative that an ET molecule is charged either slightly more

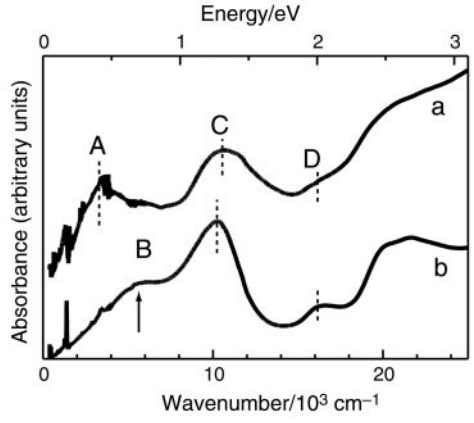

Fig. 2 Absorption spectra of $(ET)_2HCNAL$ (a) and $ET{\cdot}Br{\cdot}H_2O$ (b) in KBr. For bands A, B, C and D, see text. Arrow indicates band B in curve b.

Table 1 Crystal and refinement data for $(ET)_2HCNAL$

Chemical formula	$C_{28}H_{17}N_2O_4S_{16}$
Formula weight	958.51
Crystal system	Monoclinic
Space group	$P2/c$ (#13)
a/Å	7.606(3)
b/Å	6.773(3)
c/Å	34.531(2)
β/°	93.12(1)
V/Å^3	1776(1)
Z	2
D_c/g cm^{-3}	1.792
Diffractometer	Rigaku AFC5R
Scan mode	ω–2θ
$2\theta_{max}$/°	55
No. of intensity meas.	4741
Criterion for obs. reflection	$F_o \geqslant 1.5\sigma(F_o)$
Reflections used in LS	2449
No. of refined parameters	236
R	0.038

than +0.5 with charge delocalization or exactly +0.5 with charge localization, namely one electron per ET dimer.

According to these structural and optical results, the charge on ET is deduced to be equal or very close to +0.5 and hence the acceptor species are expected to be either $HCNAL^{(1+\delta')-}$ with δ' being equal or close to zero or a mixture of $HCNAL^{1-}$ and $CNAL^{2-}$ with the latter in nil or tiny amounts. Another possibility for the anion species is a mixture of nearly equal amounts of H_2CNAL^0 and $CNAL^{2-}$. However, this situation is the least realistic one considering that the disproponation of $HCNAL^{1-} \rightleftarrows H_2CNAL + CNAL^{2-}$ is not easy since the $pK_2 - pK_1$ is estimated to be more than 2.2,[20] where pK_1 and pK_2 mean the dissociation constants for the processes $H_2CNAL \rightleftarrows HCNAL^{1-} + H^+$ and $HCNAL^{1-} \rightleftarrows CNAL^{2-} + H^+$, respectively. As a consequence, the complex is tentatively formulated as $(ET)_2HCNAL$ in the following discussion.

3.2 Crystal and band structures

The $(ET)_2HCNAL$ complex crystallizes in the monoclinic system. The lattice parameters are summarized in Table 1. The molecular and crystal structures are shown in Fig. 3. One ET molecule and half of the HCNAL one are crystallographically unique. The ethylene groups of an ET molecule are in a staggered conformation and deviate from the least squares plane composed of the nearly planar remainder. Two ET molecules form a face-to-face dimer with a twisted overlap configuration (Fig. 3a). The dimers stack to form columns along the a-axis with interplanar distances of 3.79 and 3.42 Å (Fig. 3b). S···S contacts shorter than the sum of the van der Waals (vdW) radii (sum of vdW radii = 3.60 Å)[21] are observed (Fig. 3c) only along the side-by-side direction (3.529(2)–3.573(2) Å) to form a donor layer in the ab-plane. The packing structure of the ET molecules is classified into the α'-type in which most of the ET compounds have been assigned to be Mott insulators.[22]†

The HCNAL molecule is almost planar and produces an infinite hydrogen-bonded ribbon along the a-axis with an intermolecular O···O distance of 3.027(6) Å (Fig. 3d). The ribbons are arranged to form an anion layer in the ab-plane. The anion and donor layers stack alternately along the c-axis. The ET and HCNAL layers are connected by short atomic contacts between the end ethylene hydrogen atoms of ET and oxygen atoms of HCNAL (2.556(3)–2.594(3) Å *vs.* sum of vdW radii = 2.72 Å).

The formation of a molecular ribbon-type aggregation by

†CCDC reference number 158796. See http://www.rsc.org/suppdata/jm/b1/b101635k/ for crystallographic files in .cif or other electronic format.

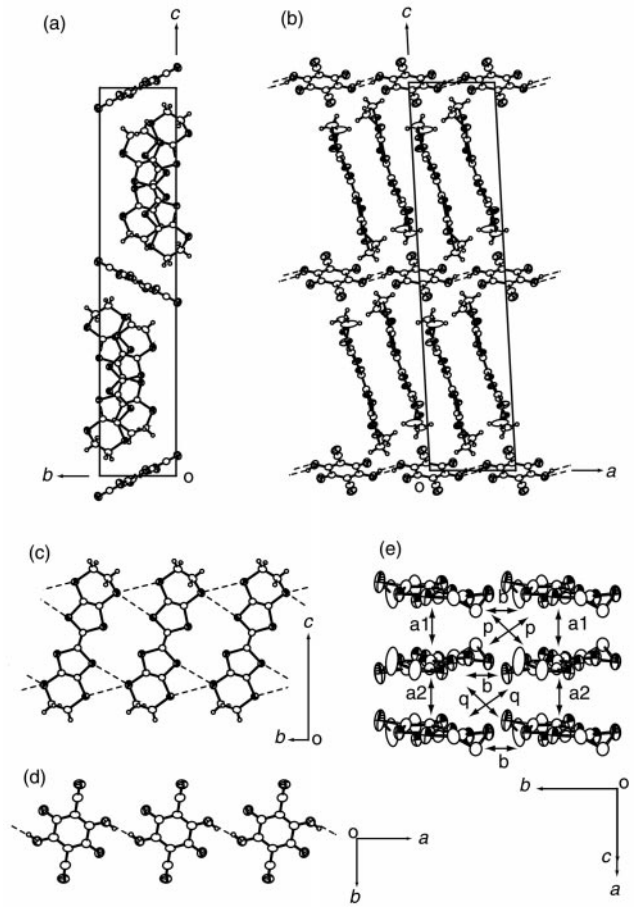

Fig. 3 Crystal structures of $(ET)_2HCNAL$ (a) viewed along the a-axis and (b) the b-axis. Hydrogen atoms are drawn as spheres of 0.1 Å radius. The hydrogen bonds between the anions are indicated by dotted lines. (c) Molecular structure of ET molecules and side-by-side S···S atomic contacts (3.529(2)–3.573(2) Å) which are shown by dashed lines. (d) Molecular structure of HCNAL and hydrogen-bonded ribbon structure of HCNAL molecules. The intermolecular O···O contacts (3.027(6) Å) are shown by dashed lines. The site occupancy factor of the phenolic hydrogen atoms is assumed to be 0.5. (e) Donor packing; letters indicate intermolecular overlap integrals; a1 = 11.53, a2 = 5.24, b = 7.37, p = 1.87, q = 2.06×10^{-3}.

complementary hydrogen-bonding has also been noted in the neutral acid (fluoranilic, chloranilic or tetrahydroxy-*p*-benzoquinone)[23] and $(TMTTF)_2HCNAL$.[12]

Fig. 4 shows the energy dispersion, density of states and the

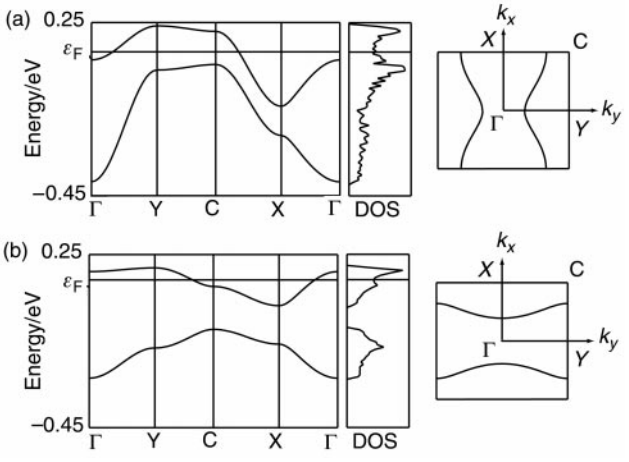

Fig. 4 Energy dispersion, density of states and Fermi surface of α'-$(ET)_2HCNAL$ calculated by extended Hückel method with tight binding approximation and single ζ-parameter (a) including or (b) excluding the d-orbitals of the sulfur atoms of the ET molecules.

Fermi surface calculated by the extended Hückel tight-binding method based on the overlap integrals including (Fig. 3e, 4a) or excluding (Fig. 4b) the 3d-orbitals of the sulfur atoms. Although the calculated band structure exhibits a strong dependency on the parameters used,[7] the Fermi level always lies in the upper branch of the dispersion as long as the degree of CT is $+0.5(1+\delta)(\delta \ll 1)$, giving rise to a quasi 1D Fermi surface open along the *a*- (Fig. 4a) or *b*- (Fig. 4b) direction despite the structural two-dimensionality of the conducting layer. The discrepancy between the directions of the open Fermi surface in Fig. 4a and 4b stems from whether the calculation includes the 3d-orbitals of sulfur or not; generally the former overestimates the overlap integrals along the *b*-direction (side-by-side direction) while the latter underestimates them. It is noteworthy that a band gap between the upper and lower HOMO bands exists in Fig. 4b but not in Fig. 4a.

3.3 Electric and magnetic properties

In spite of the presence of the Fermi surface in the band calculation, the observed temperature dependence of conductivity is semiconductive. The four-probe method shows a room temperature conductivity (σ_{RT}) of 0.20–0.83 Scm^{-1} with an activation energy of 0.15 eV (at 210–297 K) along the long axis of a single crystal (*a*-axis). The origin of the semiconductive behavior would be either (1) strong electron correlation in comparison with the band width (Mott insulator)[24] such as α′-$(ET)_2X$ (X = $CuCl_2$, $Ag(CN)_2$, $AuBr_2$, *etc.*),[22] β′-$(ET)_2X$ (X = BrICl, ICl_2, $AuCl_2$)[25] and κ-$(ET)_2Cu_2(CN)_3$[3,4] or (2) charge separation[26] such as α-$(ET)_2IBr_2$ and θ-$(ET)_2X$ (X = $RbCo(SCN)_4$, $RbZn(SCN)_4$).[27] As far as the crystal structure and IR spectrum are concerned, charge separation such as $ET^{1+} + ET^0$ is not detected experimentally. Instead, the strong electron correlation is the most plausible cause of the localization of electrons in this system (*vide infra*).

The σ_{RT} value of the title complex is comparable to those reported for the ET Mott insulators α′-$(ET)_2X$ (X = $AuBr_2$,[22b] pentacyanodicyclopentadienide(solvent)$_x$,[22e] $\sigma_{RT} = (1–5) \times 10^{-1}$ Scm^{-1}) and κ-$(ET)_2Cu_2(CN)_3$ (σ_{RT} = 3–6 Scm^{-1})[3,4] and exceeds slightly those of α′-$(ET)_2X$ (X = $CuCl_2$,[22b] $Ag(CN)_2$,[22b] IAuBr,[22c] HCl_2,[22f] *p*-$CH_3C_6H_4SO_3$,[22d] alkoxytetracyanoallylide (alkyl: methyl, ethyl, butyl),[22g] $\sigma_{RT} = 2 \times 10^{-4}–3 \times 10^{-3}$ Scm^{-1}) and β′-$(ET)_2X$ (X = ICl_2, $AuCl_2$, $\sigma_{RT} = 1–3 \times 10^{-2}$ Scm^{-1}).[25] The activation energy of 0.15 eV is comparable to those of α′- and β′-$(ET)_2X$ mentioned above (ε_a = 0.10–0.20 eV), except for the salts where X = $Ag(CN)_2$ and $AuBr_2$ (ε_a = 0.24–0.30 eV), and fairly large compared with that of κ-$(ET)_2Cu_2(CN)_3$ (0.02–0.05 eV), suggesting that α′-$(ET)_2$(HCNAL) resides well away from the boundary between Mott insulators and 10 K class superconductors in the Mott insulating side.

The definitive evidence to assign the title complex to be a Mott insulator was afforded by the magnetic measurements. The magnetic susceptibility χ of polycrystalline material was measured by a SQUID magnetometer with the external magnetic field (H_0) of 1 kOe. The temperature dependence of χ after the correction of core diamagnetism (-4.82×10^{-4} emu mol^{-1}) is shown in Fig. 5. The Curie constant (5.28×10^{-3} emu mol^{-1}) corresponds to an impurity of 1.4% of the complex. The large value of χ at room temperature (1.05×10^{-3} emu mol^{-1}) and the broad maximum at around 90 K indicate the presence of localized spins ($S = \frac{1}{2}$) coupled by antiferromagnetic interactions. It is well approximated by the 1D $S = \frac{1}{2}$ antiferromagnetic Heisenberg chain model[28] with the exchange interaction of about $J/k_B = -55$ K using the least squares method (solid line in Fig. 5), however, the position of the peak center is slightly different. To fit the peak center, it is approximated by the same model with $J/k_B = -49$ K (dashed line). Consequently, it is proper that the magnetic susceptibility is semiquantitatively approximated by the 1D antiferromagnetic Heisenberg chain model with $J/k_B = -49$ to -55 K.

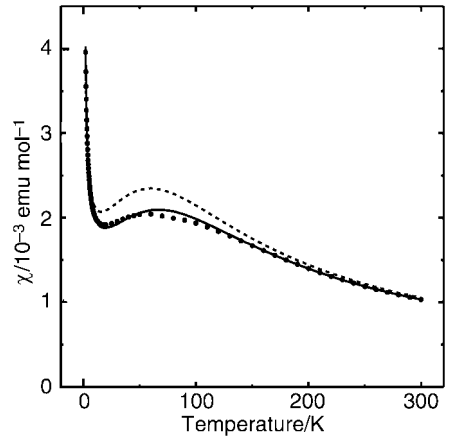

Fig. 5 Magnetic susceptibility of α′-$(ET)_2$HCNAL by SQUID after correction of Pascal diamagnetism. The Curie paramagnetism is ascribed to the defect impurity of *ca.* 1.4% of the complex. The solid and dashed curves are the fitting by the 1D Heisenberg antiferromagnet model by Bonner–Fisher with the exchange interaction of $J/k_B = -55$ K and -49 K, respectively.

The absolute value of χ at room temperature is comparable to those of the conventional α′- and β′-type ET Mott insulators ($(9–12) \times 10^{-4}$ emu mol^{-1})[22,25] and corresponds to *ca.* 82% of that of the magnetically isolated spins; the Curie law gives a χ of 1.25×10^{-3} emu mol^{-1} at 300 K when $S = \frac{1}{2}$ and $g = 2.00$.[29] The agreement between the theoretical and observed values in Fig. 5 indicates the system to be a Mott insulator with one spin per ET dimer.

The EPR measurements with the external magnetic field (H_0) perpendicular to the long axis of a single crystal indicate that a Lorentzian signal is observed solely in the temperature region above 50 K and is extinguished at lower temperatures. The temperature dependence of EPR intensity above 50 K (Fig. 6a) is qualitatively consistent with χ in Fig. 5, confirming the Bonner–Fisher type antiferromagnetic interactions. The peak-to-peak line width (H_{pp}) of the EPR signal (Fig. 6b) shows gradual broadening as temperature decreases from room temperature (H_{pp} = 4 Oe) down to 100K (7–8 Oe) then rather rapid increase below it (16–17 Oe at 50 K). The increase of H_{pp} below 100 K implies the formation of the local magnetic field caused by the growing of the antiferromagnetic order. The *g*-value (Fig. 6c) between room temperature and 100 K (2.0056–2.0062) corresponds to the molecular *g*-value of an ET cation radical.[30] The appearance of only one EPR signal with its *g*-value corresponding to the ET species confirms that

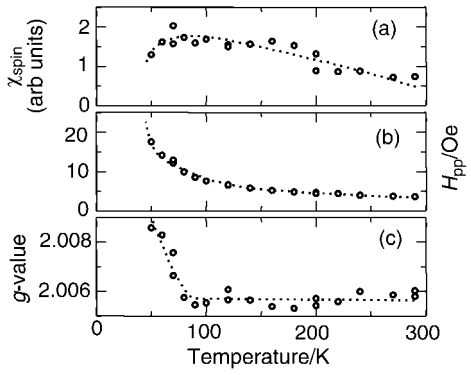

Fig. 6 Temperature dependence of (a) EPR spin susceptibility (χ_{spin}), (b) peak-to-peak line-width (H_{pp}) and (c) *g*-value of α′-$(ET)_2$HCNAL when $H_0 \perp a$. The dotted curves are guides for the eyes.

the anion species are spinless. Therefore, together with the very weak intensity of absorption band B in Fig. 2, the magnetic results indicate that an ET dimer has one localized spin to give rise to a Mott insulating state leading to a conclusion that the anion species should be an exact monoanion, $HCNAL^{1-}$.

The origin of the optical band B is anticipated as an electronic transition between the neighboring dimers. That will then be related to the on-site Coulomb repulsion of ET dimer, U_{dimer} which is approximated by eqn. (1), where ΔE is the energy splitting between upper- and lower-HOMOs of a dimer (dimerization energy).[31]

$$U_{dimer} = \Delta E + [U - (U^2 + 4\Delta E^2)^{12}]/2 \quad (1)$$

Since the on-site Coulomb repulsion U of an ET molecule is larger than ΔE of the ET molecule, U_{dimer} can be approximated by ΔE. Therefore, it is very plausible that band B appears at lower energy side than that in the Br salt (curve b in Fig. 2 indicated by an arrow) to overlap with band A in curve a in Fig. 2. These results suggest that the density of states depicted by Fig. 4b is more appropriate than that by Fig. 4a pointing out that the extended Hückel calculation including the sulfur 3d-orbitals overestimates the side-by-side interaction in the case of α'-type packing.

In conclusion, the optical, electric and magnetic measurements disclosed that the cyananilic acid H_2CNAL was deprotonated into a monoanion, $HCNAL^{1-}$, during the crystal growth by diffusion method, to form a new Mott insulator α'-$(ET)_2HCNAL$.

Acknowledgements

The authors are pleased to dedicate this article to the occasion of Professor Underhill's retirement. This research was supported by a Grant-in-Aid for Scientific Research from the Ministry of Education, Science, Sports and Culture, Japan.

References

1 T. Ishiguro, K. Yamaji and G. Saito, *Organic Superconductors*, 2nd edn, Springer-Verlag, Berlin, 1998.
2 G. Saito, A. Otsuka and A. A. Zakhidov, *Mol. Cryst. Liq. Cryst.*, 1996, **284**, 3.
3 U. Geiser, H. H. Wang, K. D. Carlson, J. M. Williams, H. A. Charlier Jr., J. E. Heindl, G. A. Yaconi, B. H. Love, M. W. Lathrop, J. E. Schirber, D. L. Overmyer, J. Ren and M. -H. Whangbo, *Inorg. Chem.*, 1991, **30**, 2586.
4 (*a*) T. Komatsu, N. Matsukawa, T. Inoue and G. Saito, *J. Phys. Soc. Jpn.*, 1996, **65**, 1340; (*b*) G. Saito, K. Ookubo, O. O. Drozdova and K. Yakushi, *Mol. Cryst. Liq. Cryst.*, in the press.
5 For some examples, see: (*a*) M. A. Beno, H. H. Wang, L. Soderholm, K. D. Carlson, L. N. Hall, L. Nunez, H. Rummens, B. Anderson, J. A. Schlueter, J. M. Williams, M.-H. Whangbo and M. Evain, *Inorg.Chem.*, 1989, **28**, 150; (*b*) H. Yamochi, C. Tada, S. Sekizaki, G. Saito, M. Kusunoki and K. Sakaguchi, *Mol. Cryst. Liq. Cryst.*, 1996, **284**, 379.
6 J. Dong, J. L. Musfeldt, J. A. Schlueter, J. M. Williams, P. G. Nixon, R. W. Winter and G. L. Gard, *Phys. Rev. B: Condens. Matter*, 1999, **60**, 4342.
7 K. Nishimura, T. Kondo, O. O. Drozdova, H. Yamochi and G. Saito, *J. Mater. Chem.*, 2000, **10**, 911.
8 G. Seitz and P. Imming, *Chem. Rev.*, 1992, **92**, 1227.
9 (*a*) D. Yoshida, H. Kitagawa, T. Mitani, T. Itoh and K. Nakasuji, *Mol. Cryst. Liq. Cryst.*, 1996, **285**, 257; (*b*) D. Yoshida, H. Kitagawa, T. Mitani, T. Itoh and K. Nakasuji, *Synth. Met.*, 1997, **86**, 2105; (*c*) K. Saito, Y. Yamaura, H. Kitagawa, D. Yoshida, T. Mitani and M. Sorai, *J. Phys. Soc. Jpn.*, 1999, **68**, 3592.
10 (*a*) T. Akutagawa, G. Saito, H. Yamochi, M. Kusunoki and K. Sakaguchi, *Synth. Met.*, 1995, **69**, 591; (*b*) T. Akutagawa, G. Saito, M. Kusunoki and K. Sakaguchi, *Bull. Chem. Soc. Jpn.*, 1996, **69**, 2487.
11 S. Horiuchi, H. Yamochi, G. Saito, K. Sakaguchi and M. Kusunoki, *J. Am. Chem. Soc.*, 1996, **118**, 8604.
12 (*a*) Md. B. Zaman, Y. Morita, J. Toyoda, H. Yamochi, G. Saito, N. Yoneyama, T. Enoki and K. Nakasuji, *Chem. Lett.*, 1997, 729; (*b*) B. Zaman, Y. Morita, J. Toyoda, H. Yamochi, S. Sekizaki and K. Nakasuji, *Mol. Cryst. Liq. Cryst.*, 1996, **287**, 249; (*c*) H. Yamochi, S. Nakamura, G. Saito, Md. B. Zaman, J. Toyoda, Y. Morita, K. Nakasuji and Y. Yamashita, *Synth. Met.*, 1999, **102**, 1729.
13 K. Wallenfels, G. Bachmann, D. Hoffmann and R. Kern, *Tetrahedron*, 1965, **21**, 2239.
14 T. Mori, A. Kobayashi, Y. Sasaki, H. Kobayashi, G. Saito and H. Inokuchi, *Bull. Chem. Soc. Jpn.*, 1984, **57**, 627.
15 P. Guionneau, C. J. Kepert, G. Bravic, D. Chasseau, M. R. Truter, M. Kurmoo and P. Day, *Synth. Met.*, 1997, **86**, 1973.
16 G. Saito, H. Izukashi, M. Shibata, K. Yoshida, L. A. Kushch, T. Kondo, H. Yamochi, O. L. Drozdova, K. Matsumoto, M. Kusunoki, K. Sakaguchi, N. Kojima and E. B. Yagubskii, *J. Mater. Chem.*, 2000, **10**, 893.
17 E. K. Andersen and I. G. K. Andersen, *Acta Crystallogr., Sect. B*, 1975, **31**, 379.
18 (*a*) T. Senga, K. Kamoshida, L. A. Kushch, G. Saito, T. Inayoshi and I. Ono, *Mol. Cryst. Liq. Cryst.*, 1997, **296**, 97; (*b*) O. O. Drozdova, V. N. Semkin, R. M. Vlasova, N. D. Kushch and E. B. Yagubskii, *Synth. Met.*, 1994, **64**, 17; (*c*) T. Hasegawa, S. Kagoshima, T. Mochida, S. Sugiura and Y. Iwasa, *Solid State Commun.*, 1997, **103**, 489.
19 T. Sugano, K. Yakushi and H. Kuroda, *Bull. Chem. Soc. Jpn.*, 1978, **51**, 1041.
20 T. Akutagawa and G. Saito, *Bull. Chem. Soc. Jpn.*, 1995, **68**, 1753.
21 A. Bondi, *J. Phys. Chem.*, 1964, **86**, 441.
22 (*a*) M. A. Beno, M. A. Firestone, P. C. W. Leung, L. M. Sowa, H. H. Wang and J. M. Williams, *Solid State Commun.*, 1986, **57**, 735; (*b*) S. D. Obertelli, R. H. Friend, D. R. Talham, M. Kurmoo and P. Day, *Synth. Met.*, 1988, **27**, A375; (*c*) A. Ugawa, K. Yakushi, H. Kuroda, A. Kawamoto and J. Tanaka, *Synth. Met.*, 1988, **22**, 305; (*d*) D. Chasseau, D. Watkin, M. J. Rosseinsky, M. Kurmoo, D. R. Talham and P. Day, *Synth. Met.*, 1988, **24**, 117; (*e*) W. H. Watson, A. M. Kini, M. A. Beno, L. K. Montgomery, H. H. Wang, K. D. Carlson, B. D. Gates, S. F. Tytko, J. Derose, C. Carris, C. A. Rohl and J. M. Williams, *Synth. Met.*, 1989, **33**, 1; (*f*) B. H. Ward, C. E. Granroth, K. A. Abboud, M. W. Meisel and D. R. Talham, *Chem. Mater.*, 1998, **10**, 1102; (*g*) S. Sekizaki, H. Yamochi and G. Saito, *Synth. Met.*, 2001, **120**, 961.
23 (*a*) H. P. Klug, *Acta Crystallogr.*, 1965, **19**, 983; (*b*) E. K. Andersen, *Acta Crystallogr.*, 1967, **22**, 188; (*c*) E. K. Andersen and I. G. K. Andersen, *Acta Crystallogr., Sect. B*, 1975, **31**, 384.
24 L. F. Mott, *Metal–Insulator Transitions*, Taylor & Francis Ltd., London, 1974.
25 (*a*) T. Enoki, J. Yamaura and A. Miyazaki, *Bull. Chem. Soc. Jpn.*, 1997, **70**, 2005; (*b*) N. Yoneyama, PhD Thesis, Tokyo Institute of Technology, Japan, 1998; (*c*) N. Yoneyama, A. Miyazaki, T. Enoki and G. Saito, *Synth. Met.*, 1997, **86**, 2029; (*d*) N. Yoneyama, A. Miyazaki, T. Enoki and G. Saito, *Bull. Chem. Soc. Jpn.*, 1999, **72**, 639.
26 H. Seo, *J. Phys. Soc. Jpn.*, 2000, **69**, 805.
27 (*a*) T. Nakamura, W. Minagawa, R. Kinami and T. Takahashi, *J. Phys. Soc. Jpn.*, 2000, **69**, 504; (*b*) H. Tajima, S. Kyoden, H. Mori and S. Tanaka, *Phys. Rev. B: Condens. Matter*, 2000, **62**, 9378; (*c*) K. Yamamoto, K. Yakushi, M. Inokuchi, M. Kinoshita and G. Saito, *Mol. Cryst. Liq. Cryst.*, in the press.
28 J. C. Bonner and M. E. Fisher, *Phys. Rev.*, 1964, **135**, A640.
29 C. Kittel, *Introduction to Solid State Physics*, 6th edn, John Wiley & Sons, Inc., New York, 1986, Ch. 14.
30 T. Sugano, G. Saito and M. Kinoshita, *Phys. Rev. B*, 1986, **34**, 117.
31 A. B. Harris and R. V. Lange, *Phys. Rev.*, 1967, **157**, 295.